# Supporting Information

## Manipulating H-bonds in Glassy Dipolar Polymers as a New Strategy for High Energy Storage Capacitors with High Pulse Discharged Efficiency

*Jingjing Liu [a], Meng Li [a], Yifei Zhao [a], Xiao Zhang [b], Junyong Lu [b], Zhicheng Zhang*[a]*

[a]Department of Applied Chemistry, Xi'an Key Laboratory of Sustainable Energy Materials Chemistry, MOE Key Laboratory for Nonequilibrium Synthesis and Modulation of Condensed Matter, School of Science, Xi'an Jiaotong University, Xi'an, P. R. China 710049.

E-mail: zhichengzhang@mail.xjtu.edu.cn

[b]National Key Laboratory of Science and Technology on Vessel Integrated Power System, Naval University of Engineering, Wuhan, P. R. China 430034.

E-mail: jylu@xinhuanet.com

**Table of Contents**

## 1. Calculation details

The discharged energy density ($U_{e,\ discharged}$) is the integral of electric field to displacement ($D$) in discharge curve of *D-E* loops tested from a Premiere II ferroelectric tester. The charged energy density and discharged efficiency should be calculated as follows,

$$U_{e,\ charged} = \int E \mathrm{d}D \qquad \text{S-1}$$

$$\eta = \frac{U_{e,discharged}}{U_{e,charged}} \times 100\% \qquad \text{S-2,}$$

where D is the displacement of dielectric tested from D-E loops, and E is the breakdown strength of the dielectric.

For the actual applied pulsed power systems, the power density and discharged energy density are evaluated by Charge-discharge instrument and calculated as follows,

$$U_e = \frac{W}{V} = \frac{\int \frac{U^2}{R} dt}{S \times d} \qquad \text{S-3}$$

$$P = \frac{U_e}{t} \qquad \text{S-4}$$

where $S$ is the electrode area, $d$ is the thickness of the film, $U$ is the voltage, $t$ is the dischare time, and $R$ is about the inset resistance (100 kΩ).

## 2. Simulation details

Atomistic molecular dynamics simulations were conducted using the software package LAMMPS,[S1] and the analysis was partially carried out using VMD.[S2] The simulations were conducted using explicit-atom Dreiding force field.[S3] The simulation cells were cubic with periodic boundary conditions in all three dimensions.

For all the samples, a single chain of P(St-MMA-MAA) with 100 backbone carbon atoms was put into a cubic cell. Each cell was replicated eight times after the energy was minimized. As a result, eight chains for each polymer were generated in the new cell at 298 K

and 1 bar, where a polymer was in an amorphous state. Samples with 0 mol%, 4 mol%, 9 mol%, 17 mol%, 25 mol% and 35 mol% MAA content (i.e., 0, 4, 9, 17, 25, and 35 MAA groups per chain, respectively) were created using the last configuration of the pure P(St-MMA) by randomly replacing -$COOCH_3$ groups with -$CH_2OH$ groups on the polymer. The equations of motion were integrated with the velocity-Verlet integrator with a time step of 1 fs.[S4,S5] Lennard-Jones and Coulombic interactions had a cut-off value of 12.5 Å. Long-range Columbic interactions were computed using the PPPM[S6] method with $10^{-6}$ accuracy. Considering the computational accuracy and expense, the model size was controlled at the maximum of ca. 12000 atoms in the models and periodic boundary conditions were applied to the cubic simulation cells. For each system, all the chosen configurations were subjected to ten - thermal annealing cycles (heating: 300–600 K, temperature interval = 50 K; cooling: 600–300 K, temperature interval= 50 K). At each temperature, a 100 ps NPT ensemble was performed at constant pressure (1 bar) with a time step of 1 fs. A Nose thermostat and Berendsen barostat were used in all the simulations. The last configuration was further subjected to a 50000 step energy minimization, followed by annealing before the system was cooled down to 300 K (temperature interval = 20 K). The 1 ns NPT simulation was applied to obtain the equilibrium density. Eventually, the 10 ns NPT and 5 ns NVT simulations were performed to collect the data. The atomic trajectory recorded every picosecond was suitable for the structural and equilibrium thermodynamic properties analysis. The simulations were conducted on a 12 core machine CPUs Intel Xeon@CPU X5650@2.67 GHz.

## 2. Figures

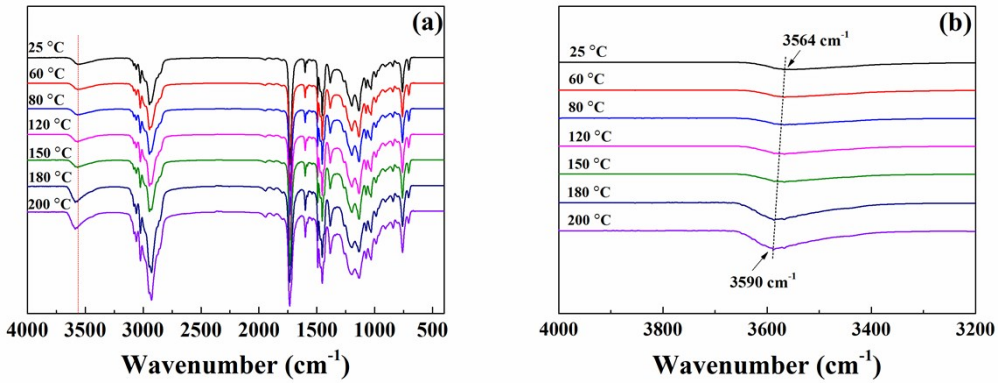


**Fig. S1.** The FTIR of P(St-MMA-MAA) (65/20/15) films at elevated temperature.

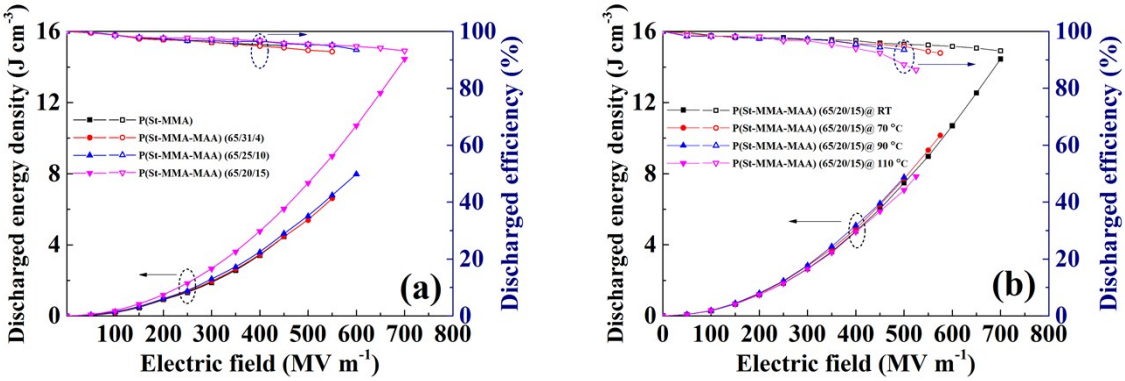


**Fig. S2.** (a) Discharged energy density and efficiency of P(St-MMA), P(St-MMA-MAA) terpolymers films at ambient temperature and (b) discharged energy density and efficiency of P(St-MMA-MAA) (65/20/15) at elevated temperatures.

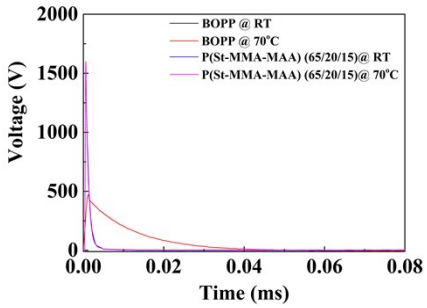


**Fig. S3.** Discharge curves of P(St-MMA-MAA) (65/20/15) and BOPP films at ambient and elevated (70 °C) temperatures.

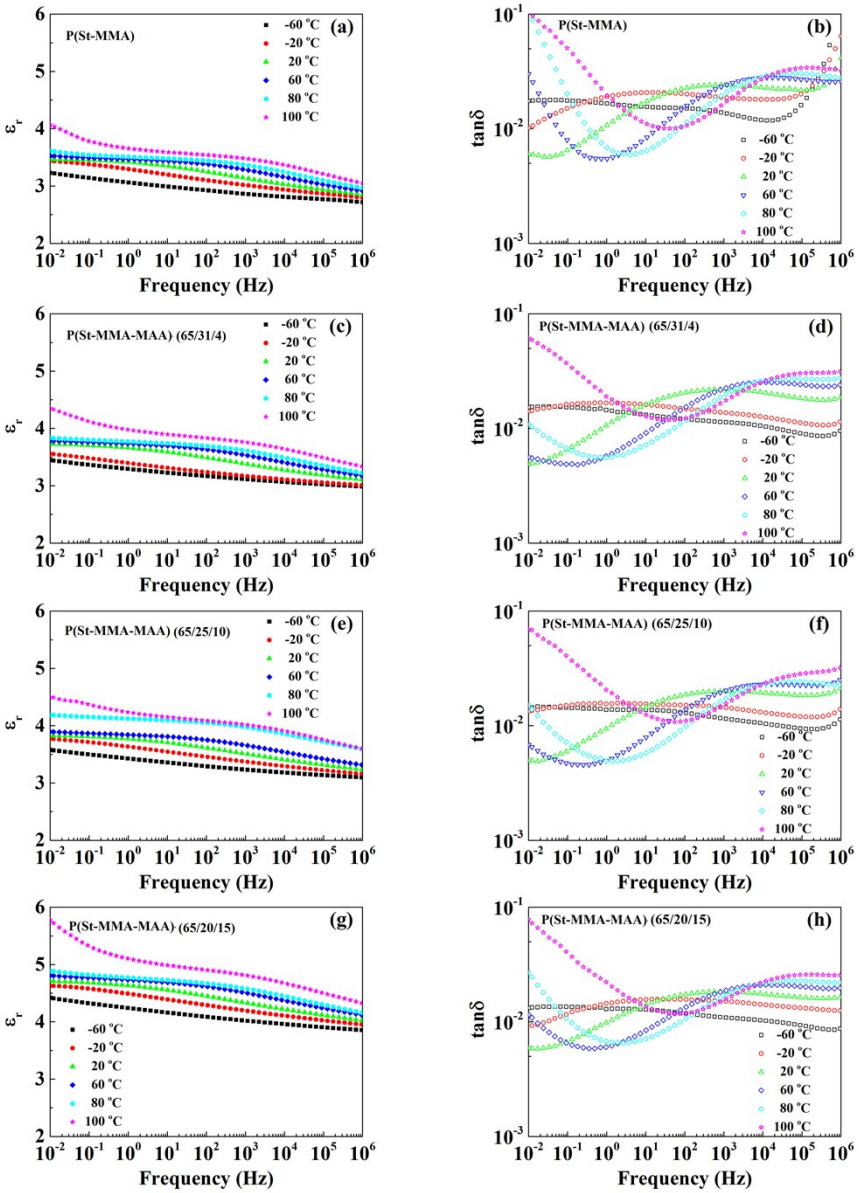


**Fig. S4.** Dielectric constant ($\varepsilon_r$) and dissipation factor (tanδ) as a function of frequency at different temperatures for P(St-MMA) and P(St-MMA-MAA)s polymers.

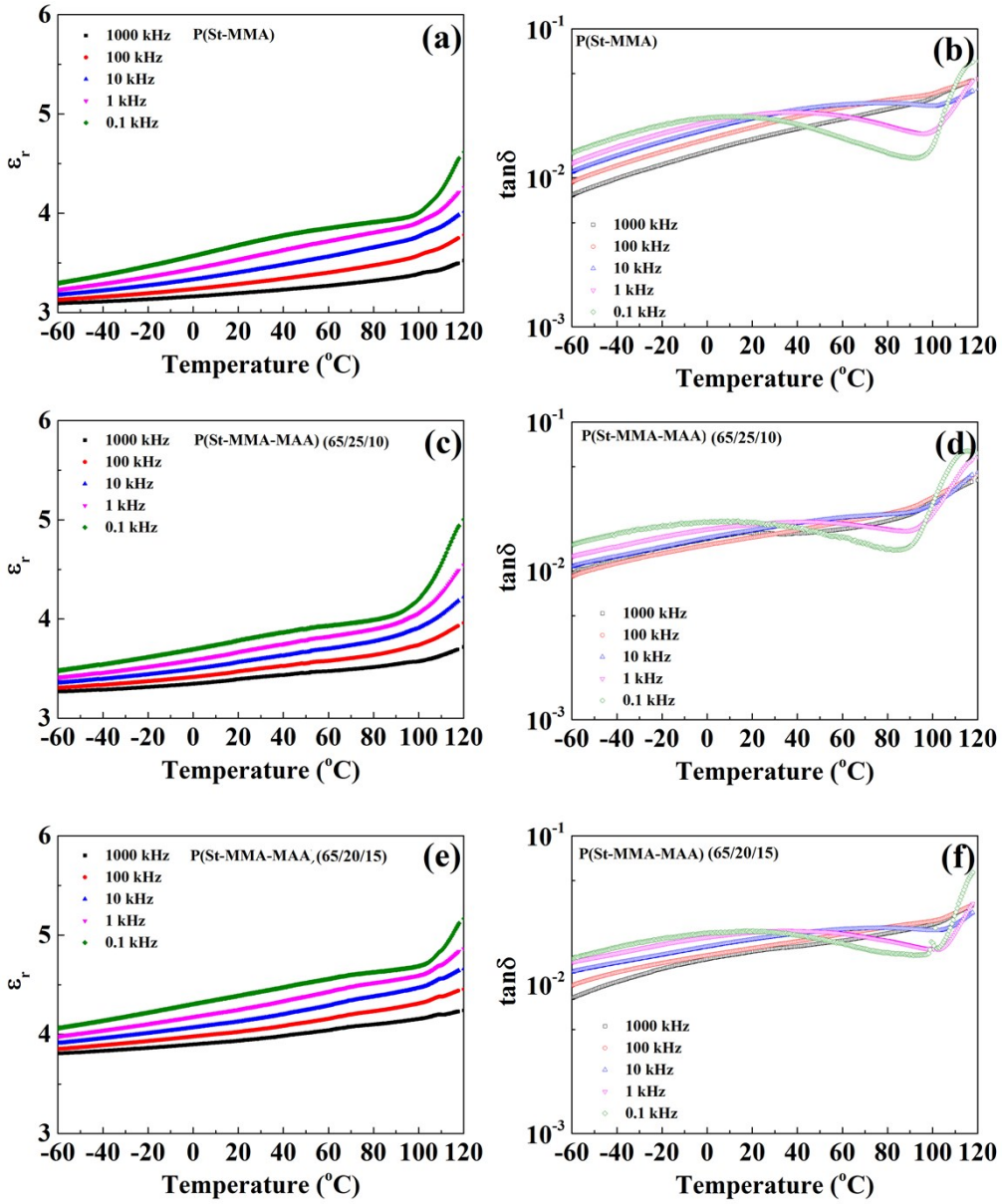


**Fig. S5.** Dielectric constant ($\varepsilon_r$) and dissipation factor (tanδ) as a function of temperature at different frequency for P(St-MMA) and P(St-MMA-MAA)s polymers.

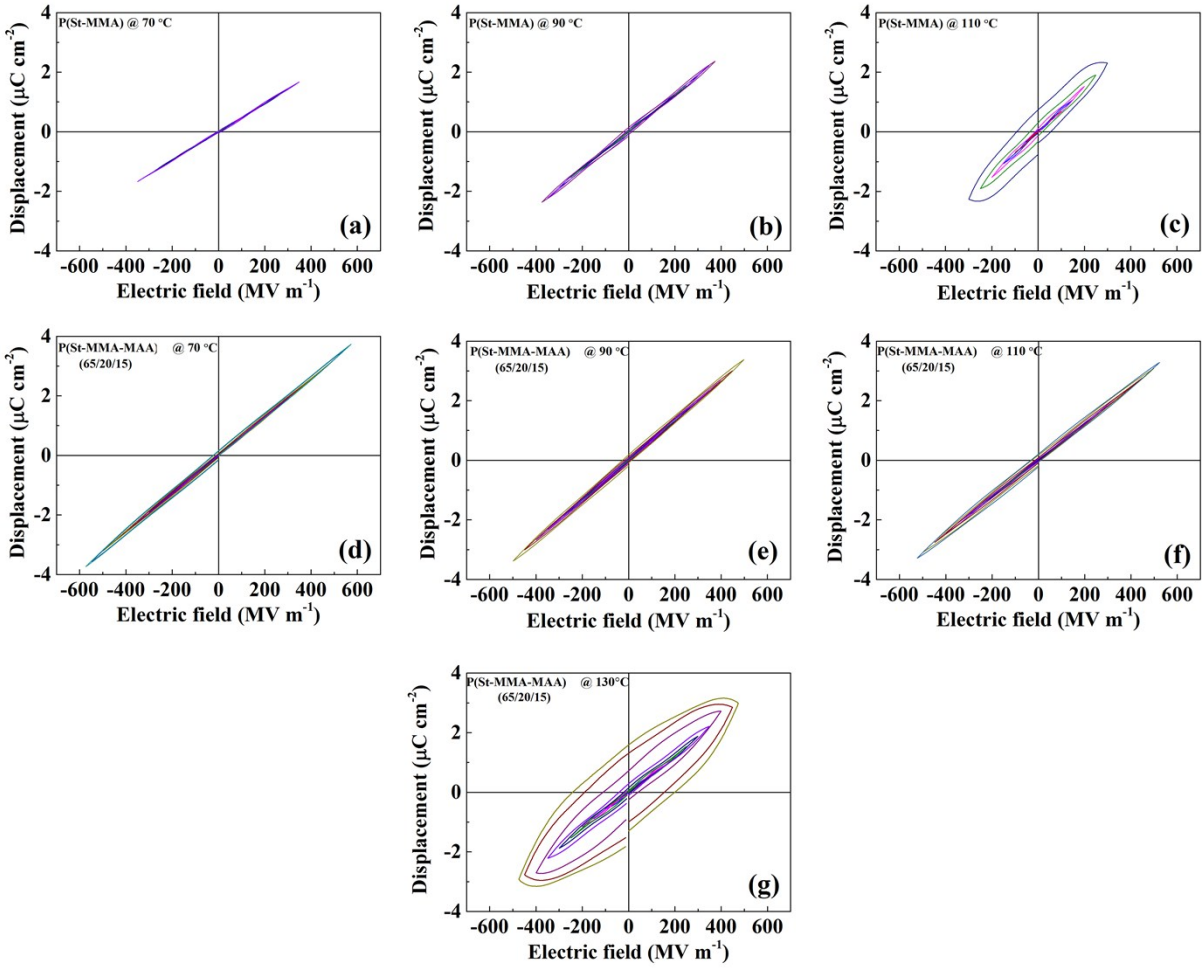


**Fig. S6.** D-E loops of P(St-MMA) and P(St-MMA-MAA) (65/20/15) films measured at elevated temperatures.

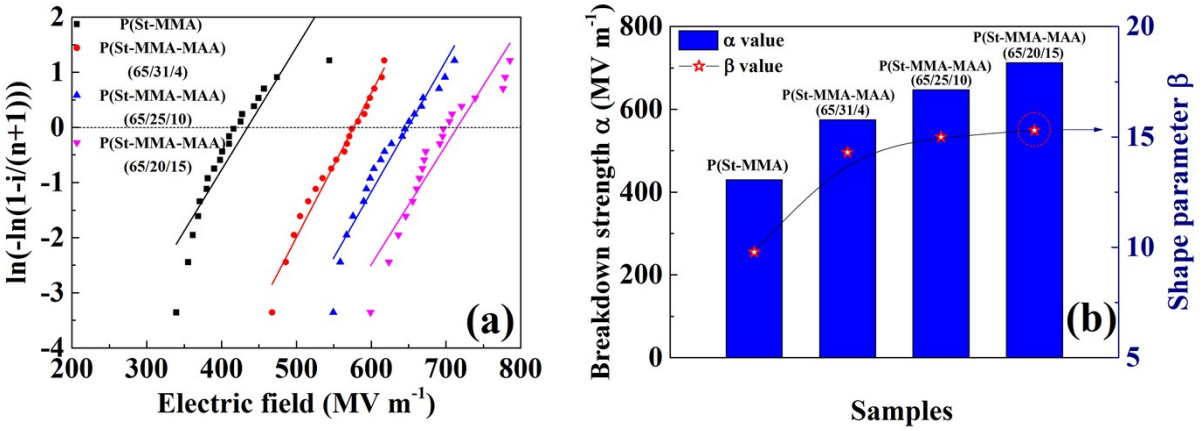


**Fig. S7.** (a) Weibull distribution of breakdown strength ($E_b$) of P(St-MMA) and P(St-MMA-MAA) films at room temperature, (b) α and β value of P(St-MMA) and P(St-MMA-MAA) films.

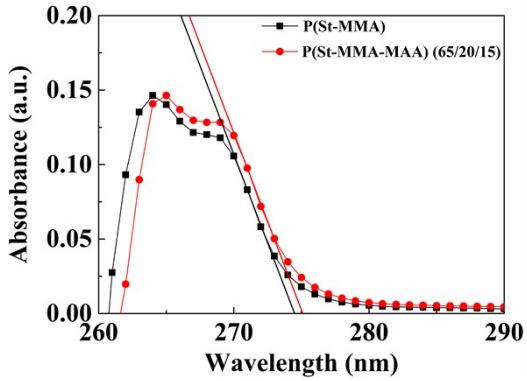


**Fig. S8.** The ultraviolet absorption spectra of P(St-MMA) and P(St-MMA-MAA) (65/20/15).

The band gaps of P(St-MMA) and P(St-MMA-MAA) (65/20/15) could be calculated from the equation,

$$E=hc / \lambda=1240 / \lambda \quad \text{S-5}$$

where $h$ is the Planck's constant, $c$ is the speed of light, and $\lambda$ is the onset value of the absorption spectrum in the long wavelength region.[S10] The band gaps of P(St-MMA) and P(St-MMA-MAA) (65/20/15) are 4.52 eV and 4.50 eV respectively. According to the literature, [S11-13] the band gap over 4.0 eV is sufficient for dielectrics to achieve high breakdown strength.

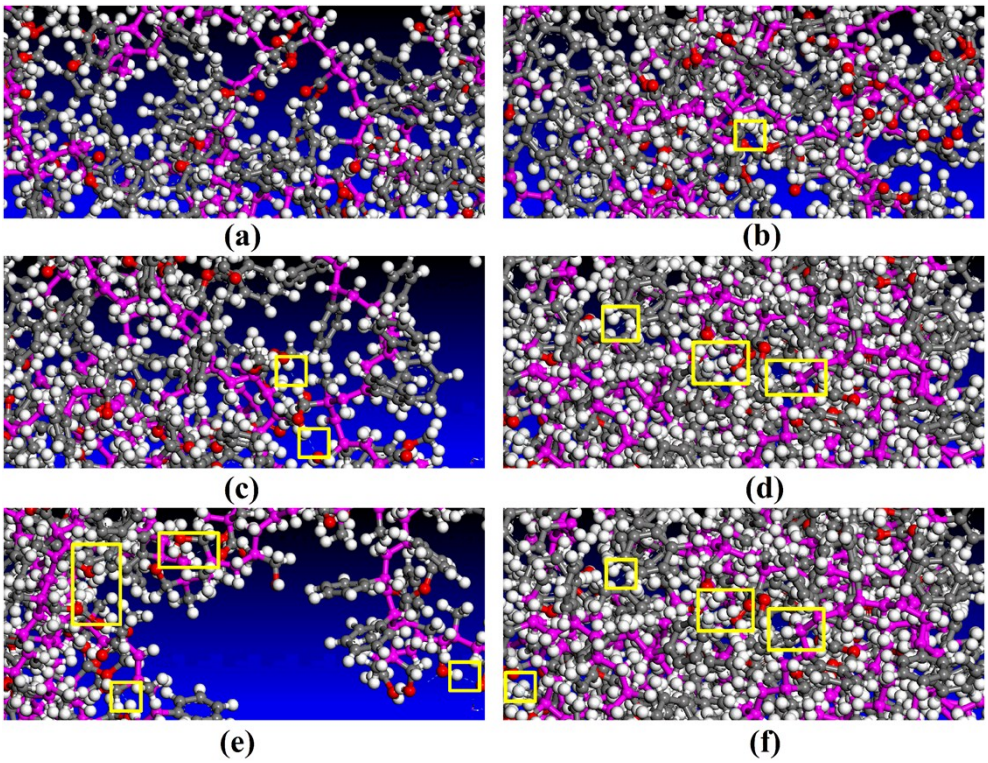

**Fig. S9.** Simulation snapshots of 0 mol % (a), 4 mol % (b), 9 mol % (c), 17 mol % (d), 25 mol % (e) and 35 mol% (f) MAA-containing terpolymers. The oxygen, hydrogen, and carbon atoms are shown as red, white and gray spheres, respectively. The polymer main chain is denoted by purple color. The yellow box highlights the H-bonds (cyan dotted line) formed in terpolymers.

# 3. Tables

**Table S1.** Selected examples of dielectric polymers and their capacitive performance.

| Polymer | $\varepsilon_r$ (1 kHz) | | | E (450 MV m$^{-1}$) | | $U_{emax}$ (J cm$^{-3}$) | $\eta_{max}$ | Ref.[d] |
|---|---|---|---|---|---|---|---|---|
| | 25 °C | 70 °C | 110 °C | $U_e$ (J cm$^{-3}$) | $\eta$ | | | |
| PP | 2.2 | 2.2 | 2.2 | 2.2 | 91% | 4 @ 600 MV m$^{-1}$ | 87% | [S7] |
| BOPP | 2.2 | 2.2 | 2.2 | 2.6 | 96% | 4.4 @ 650 MV m$^{-1}$ | 83% | [29] |
| BOPP | 2.2 | - | - | 1.6[b] | 97%[b] | 1.63 @ 400 MV m$^{-1}$[c] | 93%[c] | [13] |
| PP-OH | 4.6 | 4.7 | - | 4.3 | - | 7 @ 650 MV m$^{-1}$ | - | [12] |
| $SO_2$-PPOs | 8 | 8.4 | 9 | 8 | 92% | 21 @ 700 MV m$^{-1}$ | 85% | [15] |
| ArPTU | 4.4 | 4.2 | 4.2 | 4.2 | 95% | 10 @ 700 MV m$^{-1}$ | 94% | [29] |
| PPEK | 3.4 | 3.3 | 3.2 | 3.8 | 97% | | - | [26] |
| PEKK | 3.55 | 3.45 | 3.4 | 2.9 | 90% | | - | [25] |
| PEEU | 4.7 | 4.5 | 4.3 | 13 | 85% | | - | [30] |
| PMSEMA | 10 | 12 | 20 | 4.54[a] | 80% [a] | | - | [27] |
| X-PP | 3 | 3 | 2.9 | - | - | | - | [S8] |
| OA-10G | 5.7 | 5.7 | 5.7 | - | - | - | - | [S9] |

[a]The $U_e$ and $\eta$ at 283 MV m$^{-1}$. [6]The $U_e$ and $\eta$ at 400 MV m$^{-1}$. [c]The $U_e$ and $\eta$ at 400 MV m$^{-1}$ and 70°C. [d]References are listed in the manuscript and supporting information.

**Table S2.** Chemical compositions and physical parameters of the parent P(St-MMA) and P(St-MMA-MAA) polymers.

| Entry | $LiAlH_4$ [mmol] | St/MMA/MAA[a] | $T_g$ [°C] | $E_s$[b] [MPa] | $E_L$[c] [MPa] | $E_T$[d] [MPa] |
|---|---|---|---|---|---|---|
| P(St-MMA) | 0 | 65/35/0 | 106 | 2549.7 ± 178.5 | 42.1 ± 3.4 | 1183.3 ± 82.8 |
| P(St-MMA-MAA) (65/31/4) | 2.1 | 65/31/4 | 110 | 2651.5 ± 265.2 | 99.6 ± 8.0 | 1446.5 ± 130.2 |
| P(St-MMA-MAA) (65/25/10) | 2.6 | 65/24/11 | 114 | 3221.0 ± 289.9 | 122.2 ± 11.0 | 2209.9 ± 221.0 |
| P(St-MMA-MAA) (65/20/15) | 3.1 | 65/20/15 | 121 | 3686.8 ± 258.1 | 134.6 ± 9.4 | 2769.5 ± 221.6 |
| P(St-MMA-MAA) (more MAA content) | 3.6 | Gel | - | - | - | - |

Reaction conditions: P(St-MMA) (2g) and $LiAlH_4$ in anhydrous THF (80 mL) for 48 h under $N_2$ atmosphere at ambient temperature. [a]The molar ratio of St/MMA/MAA was determined by $^1$H NMR. [b]The storage modulus and [c]loss modulus of samples were determined by DMA at 30 °C. [d]The tensile modulus of samples was calculated using tensile testing.

## References


S1. S. Plimpton, *J. Comput. Phys.* 1995, **117**, 1-19.

S2. W. Humphrey, A. Dalke, K. Schulten, *J. Mol. Graph.* 1996, **14**, 33-38.

S3. S. L. Mayo, B. D. Olafson, W. A. Goddard, *J. Phys. Chem.* 1990, **94**, 8897-8909.

S4. L. Verlet, *Phys. Rev.* 1967, **159**, 98.

S5. L. Verlet, *Phys. Rev.* 1968, **165**, 201.

S6. J. W. Eastwood, R. W. Hockney, D. N. Lawrence, *Comput. Phys. Commun.* 1980, **19**, 215.

S7. M. Rabuffi, P. Guido, *IEEE Trans. Plasma Sci.* 2002, **30**, 1939-1942.

S8. X. P. Yuan, T. C. M. Chung, *Appl. Phys. Lett.* 2011, **98**, 062901.

S9. N. J. Smith, B. Rangarajan, M. T. Lanagan, C. G. Pantano, *Mater. Lett.* 2009, **63**, 1245-1248.

S10. C. Zhang, Y. P. Zang, F. J. Zhang, Y. Diao, C. R. McNeill, C. A. Di, X.Z. Zhu, D. B. Zhu,. *Adv. Mater.*, 2016, **28**, 8456-8462.

S11. Z. Z. Li, G. M. Treich, M. Tefferi, C. Wu, S. Nasreen, S. K. Scheirey, R. Ramprasad, G. A. Sotzing, Y. Cao, *J. Mater. Chem. A*, 2019, **7**, 15026-15030.

S12. E. Baer, L. Zhu, *Macromolecules*, 2017, **50**, 2239-2256.

S13. C. C. Wang, G. Pilania, S. A. Boggs, S. Kumar, C. Breneman, R. Ramprasad, *Polymer*, 2014, **55**, 979-988.